Semi-classical Anharmonic Correlated Einstein Model Debye–Waller Factors and EXAFS of Hcp Crystals

N.C. Toan and N.V. Hung*

Department of Physics, VNU University of Science, 334 Nguyen Trai, Thanh Xuan, Hanoi, Vietnam

Received: 05.04.2023 & Accepted: 27.04.2023

Doi: 10.12693/APhysPolA.144.38 *e-mail: hungnv@vnu.edu.vn

A semi-classical anharmonic correlated Einstein model of hcp crystals is derived for the high-order expanded Debye–Waller factors and extended X-ray absorption fine structure. The many-body effect is included in this model based on the contributions of the first shell near neighbors of the absorber and backscatter atoms. The analytical expressions of Debye–Waller factors presented in terms of cumulant expansion up to the fourth order yield results based on the classical theory corrected for its absence of zero-point vibration. The anharmonic many-body effect effective potential is derived which includes the Morse potential for describing the single-pair atomic interactions. A method of providing all extended X-ray absorption fine structure quantities is created, correcting the absence of zero-point vibration in classical theory, combining it with the quantum one based on only the second cumulant. The derived model has the advantage of including both classical and quantum effects. The numerical results of all considered quantities of Zn (hcp) are found to be in good agreement with the experimental values.

topics: semi-classical anharmonic correlated Einstein model, Debye–Waller factor and extended X-ray absorption fine structure (EXAFS), anharmonic effective potential and cunulant expansion, hexagonal close-packed (hcp) crystals

1. Introduction

The thermal atomic vibrations and disorder in extended X-ray absorption fine structure (EXAFS) give rise to the Debye–Waller factor (DWF), which damps EXAFS spectra with respect to increasing temperature T and wave number k (energy). The anharmonicity in atomic interaction potential yields additional terms in DWF, which, when ignored, can lead to non-negligible errors in structural parameters [1–26]. The formalism for including anharmonic effects in EXAFS is often based on the cumulant expansion approach [1], where the even cumulants contribute to the amplitude and the odd ones to the phase of EXAFS spectra. The accurate DWFs, due to their exponential damping, are crucial to the quantitative treatment of EXAFS. Consequently, the lack of precise DWFs has been one of the biggest limitations to accurate structural determinations (e.g., the coordination numbers and the atomic distances) and specifying different physical parameters [21, 26] from EXAFS data.

In order to overcome the above limitations, several procedures based on classical and quantum theories have been developed for studying the DWFs, including anharmonic contributions or phonon–phonon interactions for different material systems using the cumulant expansion approach [1–26], where for small anharmonicities, it is sufficient to keep the third and fourth cumulants [2]. At high temperatures, the classical approaches, for example, the classical single-bond model (CSBM) [3] and some methods for studying the anharmonic effects in EXAFS [4–7], work well. But they are limited at low temperatures due to the absence of zero-point vibration. Several quantum methods have been derived for approximating the EXAFS cumulants, for example, the quantum single bond models [8, 9], the full lattice dynamical (FLD) approach [10], the anharmonic correlated Einstein model (ACEM) [11], the pressure-dependent ACEM [12], as well as the ACEMs for studying EXAFS of doping materials compared to Mössbauer studies [13], and the isotopic [14] effects in EXAFS of the considered crystals, as well as the thermal properties of semiconductors [15, 16]. The further efforts in these developments are expressed by the path integral effective potential model [17], the force constant method [18, 19], the path-integral Monte Carlo procedure [20], the dynamic matrix calculation [21], and the density functional theory for DWF [22]. Moreover, recently the DWF-based

methods for studying the strong anharmonicity in tin monosulfide evidenced by local distortion, high-energy optic phonons [23], and the melting curve, eutectic point, and Lindemann's melting temperature of hcp binary alloys [24] have been published. The advantages of the classical methods are simplicity and usefulness in describing the dominant anharmonicity at high temperatures, even at melting temperatures [3]. The quantum models have the advantage of being well-suited to describe the quantum effects at low temperatures based on including the zero-point energy contributions. Therefore, it is very useful to combine the classical models with the quantum ones, obtaining a semi-classical ACEM (SCACEM), which has the advantages of both classical and quantum theories.

The purpose of this work is to derive a SCACEM for hcp (hexagonal close-packed) crystals, combining a classical model with a quantum one for the calculation and analysis of the high-order expanded DWFs describing the thermodynamic properties and anharmonic effects, as well as anharmonic EXAFS contributing to the accurate structural determination. In Sect. 2, the derivation of the present SCACEM is presented. An anharmonic many-body effect effective potential is derived instead of the single-pair potential (SPP) used elsewhere [3, 8–10]. The Morse potential is adopted to describe the single-pair atomic interactions. The many-body effect is taken into account in a simple manner based on the contributions of the first shell near neighbors of the absorber and backscatter atoms. The analytical expressions of DWFs presented in terms of cumulant expansion up to the fourth order yield results based on the classical theory corrected for its absence of zero-point vibration. The method is created to:

- indicate the best way of providing all considered EXAFS quantities;
- correct the absence of zero-point vibration in a classical EXAFS theory;
- combine the classical theory with the quantum one, with the advantage of realizing these purposes based on only the second cumulant or mean square relative displacement (MSRD).

Furthermore, the equality of the obtained relation $\sigma^{(1)}\sigma^2/\sigma^{(3)}$ among the first $\sigma^{(1)}$, second σ^2, and third $\sigma^{(3)}$ cumulants to the classical value of $1/2$ [3] at all temperatures, while these obtained cumulants contain the zero-point energy contributions, leads to a conclusion that the derived SCACEM includes both classical and quantum effects. In Sect. 3, the anharmonic EXAFS of hcp crystals is studied based on the obtained SCACEM cumulants. The numerical results (Sect. 4) of all considered quantities (cumulants, EXAFS spectra and their Fourier transform magnitudes) of Zn in the hcp phase are compared to the experimental values measured at HASYLAB (DESY, Germany) published elsewhere [7, 25], as well as to those measured at the BL8, Synchrotron Light Research Institute (SLRI, Thailand) [26]. The significant discrepancies between the results calculated by the CSBM [3] and by the present method using the SPPs, indicate the limitations of the SPP model. The conclusions on the obtained results are presented in Sect. 5.

2. Semi-classical ACEM (SCACEM) of hcp crystals

2.1. Anharmonic and many-body effects in SCACEM

The anharmonic contributions and many-body effects included in the present SCACEM of hcp crystals are considered based on an anharmonic many-body effect effective potential expanded up to the fourth order as a function of the displacement $x = r - r_0$ along the bond direction with r and r_0 being, respectively, the instantaneous and equilibrium distances between absorber and backscatter atoms, i.e.,

$$V_{\text{eff}}(x) \cong \frac{1}{2} k_{\text{eff}}\, x^2 + k_{3\text{eff}}\, x^3 + k_{4\text{eff}}\, x^4, \tag{1}$$

where k_{eff} is the effective local force constant, and $k_{3\text{eff}}$ and $k_{4\text{eff}}$ are the effective parameters describing the anharmonic effects giving the asymmetry of the derived effective potential.

Based on the center-of-mass frame of single-bond pair of absorber and backscatter atoms [11], the anharmonic effective potential given by (1) has been defined as

$$V_{\text{eff}}(x) = V(x) + \sum_{i=1,2} \sum_{j \neq i} V\left(\frac{\mu\, x}{M_i} \hat{\boldsymbol{R}}_{12} \cdot \hat{\boldsymbol{R}}_{ij}\right) = V(x) + M(x), \tag{2}$$

where

$$M(x) = 2V\left(-\frac{x}{2}\right) + 8V\left(-\frac{x}{4}\right) + 8V\left(\frac{x}{4}\right). \tag{3}$$

Note that V_{eff} is the sum of not only the term $V(x)$ describing the pair-interaction between absorber and backscatter atoms, but also the term $M(x)$ consisting of the components $2V(x/2)$, $8V(x/4)$ and $8V(-x/4)$ given by (3), describing the projections of their pair-interactions with the first shell near neighbors along the bond direction, where $\mu = M_1 M_2/(M_1 + M_2)$ is reduced mass of absorber with mass M_1 and backscatter with mass M_2, $\hat{\boldsymbol{R}}$ is a unit vector. The sum for the index i is for absorber ($i = 1$) and backscatter ($i = 2$). The sum for j is for all first shell near neighbors, where the first line in (2) is for any structure, and the second one is valid for monatomic hcp crystals.

The term $M(x)$ given in (3) actually describes the lattice contributions or many-body effects to the pair-interaction of absorber and backscatter atoms of hcp crystals whose vibration behaves as a linear anharmonic oscillator in the present SCACEM.

Applying the Morse potential expanded up to the fourth order

$$V(x) = D\left(\mathrm{e}^{-2\alpha x} - 2\mathrm{e}^{-\alpha x}\right) \cong$$

$$D\left(-1 + \alpha^2 x^2 - \alpha^3 x^3 + \frac{7}{12}\alpha^4 x^4\right) \tag{4}$$

to (2)–(3), as well as comparing the results to (1), we obtain the effective parameters $k_{\mathrm{eff}}, k_{3\mathrm{eff}}, k_{4\mathrm{eff}}$ for hcp crystals in terms of Morse potential parameters D and α as follows

$$k_{\mathrm{eff}} = 5D\alpha^2, \qquad k_{3\mathrm{eff}} = -\frac{5}{4}D\alpha^3,$$

$$k_{4\mathrm{eff}} = \frac{133}{192}D\alpha^4. \tag{5}$$

These parameters are quite different from those of SPP, which include only the term $V(x)$, written below

$$k_{\mathrm{SPP}} = 2D\alpha^2, \qquad k_{3\mathrm{SPP}} = -D\alpha^3,$$

$$k_{4\mathrm{SPP}} = \frac{7}{12}D\alpha^4, \tag{6}$$

where D is dissociation energy and α describes the width of the potential.

2.2. Classical ACEM (CACEM) including many-body effect

The first step of deriving the present SCACEM is advancing a classical model like the well-known CSBM [3] into the classical ACEM (CACEM) based on the high-order expanded DWFs, including the many-body effect. The derivation of such DWFs is based on the cumulant expansion approach [1] and the classical statistical theory, treating the anharmonicity as a perturbation and the temperature-dependence of the moments about the mean $\langle x\rangle$ to the lowest orders in temperature T, as determined by evaluating the thermal average

$$\left\langle \left(x - \langle x\rangle\right)^n \right\rangle = \frac{\int\limits_{-\infty}^{\infty} \mathrm{d}x\,(x - \langle x\rangle)^n \exp\left(-\frac{V_{\mathrm{eff}}(x)}{k_{\mathrm{B}}T}\right)}{\int\limits_{-\infty}^{\infty} \mathrm{d}x\,\exp\left(-\frac{V_{\mathrm{eff}}(x)}{k_{\mathrm{B}}T}\right)}, \tag{7}$$

which uses the high-order expanded anharmonic effective potentials $V_{\mathrm{eff}}(x)$ given by (1)–(3) instead of SPP used in CSBM [3].

The truncation of the series calculated from (7) serves as a convergence cutoff while including enough terms to accurately obtain the second lowest-order expressions for the moments. From these results, including the anharmonic effective potential parameters $k_{\mathrm{eff}}, k_{3\mathrm{eff}}, k_{4\mathrm{eff}}$ given by (5) for hcp crystals to lowest order in temperature T, the temperature-dependent expressions in terms of Morse potential parameters have resulted for the second cumulant describing MSRD

$$\sigma^2(T) = \langle (r - r_0)^2\rangle \cong \langle x^2\rangle = \frac{k_{\mathrm{B}}T}{5D\alpha^2}. \tag{8}$$

The first cumulant describing the net thermal expansion or lattice disorder is

$$\sigma^{(1)}(T) = \langle r - r_0\rangle = \langle x\rangle = \frac{3}{4}\alpha\,\sigma^2(T). \tag{9}$$

The third cumulant or mean cubic relative displacement (MCRD) describing the asymmetry of the pair distribution function is

$$\sigma^{(3)}(T) = \left\langle (r - r_0)^3\right\rangle \cong$$

$$\left\langle x^3\right\rangle - 3\sigma^{(1)}\sigma^2 = \frac{3}{2}\alpha\left(\sigma^2(T)\right)^2. \tag{10}$$

The fourth cumulant describing the anharmonic contribution to EXAFS amplitude is

$$\sigma^{(4)}(T) = \langle (r - r_0)^4\rangle - 3\left(\sigma^2\right)^2 =$$

$$\frac{137}{40}\alpha^2\left(\sigma^2(T)\right)^3, \tag{11}$$

and the relation among the three first EXAFS cumulants is given by

$$\frac{\sigma^{(1)}\sigma^2}{\sigma^{(3)}} = \frac{1}{2}. \tag{12}$$

The atomic vibration is characterized by its frequency so that using the obtained effective local force constant k_{eff}, the correlated Einstein frequency ω_{E}, and temperature θ_{E} have resulted in

$$\omega_{\mathrm{E}} = \sqrt{\frac{5D\alpha^2}{\mu}}, \quad \theta_{\mathrm{E}} = \frac{\hbar\omega_{\mathrm{E}}}{k_{\mathrm{B}}}, \tag{13}$$

where μ is the reduced mass of absorber and backscatter atoms, k_{B} is Boltzmann constant.

Note that the application of the anharmonic effective potential parameters $k_{\mathrm{eff}}, k_{3\mathrm{eff}}, k_{4\mathrm{eff}}$ to the obtained cumulant expressions instead of the SPP ones in the above derivation of the high-order expanded DWFs is shown actually as the first improvement by including the many-body effects in these quantities, making CSBM [3] the present CACEM. Moreover, the presentation of the obtained cumulants given by (8)–(11) in terms of second cumulant $\sigma^2(T)$ leads to the creation of a method that provides all considered quantities based on only the second cumulant or MSRD, giving a significant reduction and simplification of the numerical calculations, the great advantage of which is shown in Sect. 4. This created method also provides the best way of correcting the absence of zero-point vibration in the classical theory of EXAFS and combining it with the quantum one performed in Sect. 2.3.

2.3. Combination of CACEM with quantum model leading to SCACEM

The further improvement making the obtained CACEM the SCACEM of hcp crystals is combining CACEM with a quantum one of hcp crystals [25], correcting the absence of zero-point energy contributions in all quantities that existed in every

TABLE I

The values k_S, k_{3S}, k_{4S}, $\omega_{\mathrm{E}S}$, $\theta_{\mathrm{E}S}$ of Zn calculated for the effective (S = eff) and single-pair (S = SSP) potentials using the Morse potential parameters [28] compared to experimental ones (S = expt.) [25].

S	k_S [N/m]	k_{3S} [eV/Å^3]	k_{4S} [eV/Å^4]	$\omega_{\mathrm{E}S}$ ($\times 10^{13}$) [Hz]	$\theta_{\mathrm{E}S}$ [K]
eff (present)	39.5616	−1.0528	0.9949	2.6917	205.6101
expt. [25]	39.0105	−1.0348	0.9749	2.6729	204.1730
SPP	15.8247	−0.8422	0.8378	1.7024	130.0392

classical model, including the present CACEM based on replacing the classical second cumulant given by (8) by the quantum one

$$\sigma^2 = \sigma_0^2 \frac{1+z(T)}{1-z(T)}, \quad \sigma_0^2 = \frac{\hbar\omega_{\mathrm{E}}}{10D\alpha^2},$$

$$z(T) = \exp\left(-\theta_E/T\right), \tag{14}$$

where $z(T)$ is temperature variable.

In this SCACEM, the expressions of the first $\sigma^{(1)}$, third $\sigma^{(3)}$, and fourth $\sigma^{(4)}$ cumulants remain the expressions given by (9)–(11), respectively. Then, it is possible for the obtained SCACEM to include not only the dominant anharmonicity at high temperatures, the advantage of a classical model like CSBM [3], but also the zero-point energy contributions at low temperatures like in [25], the advantage of a quantum model.

Note that the derived SCACEM of hcp crystals is an effective and useful combination of a classical model of EXAFS with a quantum one where the zero-point energy contribution σ_0^2 of the second cumulant given by (14), based on the above-created method by automatically entering the expressions of the other cumulants given by (9)–(11) corrects their absence of zero-point vibration. The interesting result obtained here is that the cumulant relation $\sigma^{(1)}\sigma^2/\sigma^{(3)}$ of SCACEM is equal to the classical value of $1/2$ at all temperatures as a classical effect [3], while the cumulants included in this relation contain the zero-point energy contributions, a quantum effect. This demonstrates the advantage of SCACEM of including both classical and quantum effects.

3. Anharmonic EXAFS of hcp crystals based on SCACEM

Further, for studying the anharmonic EXAFS of hcp crystals based on the present SCACEM and the cumulant expansion approach [1], the analytical expression of the temperature-dependent K-edge anharmonic EXAFS spectra is derived and given by

$$\chi(k,T) = \sum_j \frac{S_0^2 N_j}{kR_j^2} \sin\left(2kR_j + \Phi_j(k) + \Phi_A^j(k,T)\right) \times F_j(k)\, F_A(k,T)\ \mathrm{e}^{-\left(2k^2\sigma^2(T) + 2R_j/\lambda(k)\right)}, \tag{15}$$

where S_0^2 is the square of the many body overlap term, N_j is the atomic number of each shell, $\Phi(k)$ is net phase shift, the mean free path λ is defined by the imaginary part of the complex photoelectron momentum $p = k + i/\lambda$, and the sum for j includes all considered atomic shells.

The expression for the anharmonic EXAFS given by (15) differs from the one of the harmonic model [27] by including the above obtained SCACEM cumulants, which lead to the factors describing the temperature T- and photoelectron wave number k-dependence of the anharmonic contributions to the amplitude

$$F_A(k,T) = \exp\left[-\frac{2}{3}k^3\sigma^{(4)}(T)\right], \tag{16}$$

and to the phase

$$\Phi_A(k,T) \cong -4k\left[\sigma^2(T)\left(\frac{1}{R}+\frac{1}{\lambda}\right) + \frac{1}{3}\sigma^{(3)}(T)\,k^2\right], \tag{17}$$

of the anharmonic EXAFS spectra of hcp crystals which are attenuated due to the factor $F_A(k,T)$ and phase shifted by the term $\Phi_A(k,T)$ compared to the harmonic ones.

4. Numerical results and discussions

Now, the expressions derived in the previous sections are applied to numerical calculations of the considered EXAFS quantities of Zn in the hcp phase using its Morse potential parameters [28] D = 0.1698 eV, $\alpha = 1.7054$ Å^{-1}. The local force constant k_S, anharmonic parameters k_{3S}, k_{4S}, correlated Einstein frequency $\omega_{\mathrm{E}S}$, and temperature $\theta_{\mathrm{E}S}$ for the anharmonic effective (S = eff) and single-pair (S = SPP) potentials of Zn have been calculated. Some results are given in Table I and compared with the experimental ones (S = expt.) obtained from the measured Morse parameters (MMP) [25] $D = 0.1685$ eV, $\alpha = 1.7000$ Å^{-1}.

Figure 1 illustrates the anharmonic many-body effect effective potential $V_{\mathrm{eff}}(x)$ of Zn calculated using the present theory (SCACEM). It has been found to be in good agreement with the experimental values (expt.) [25] and asymmetric compared to the harmonic term due to the inclusion of the anharmonic contributions.

TABLE II

Comparison of the values of four first EXAFS cumulants of Zn calculated using the present theory (SCACEM) with their experimental values (expt.) at 77, 300, 400, 500, and 600 K. The experimental values at 77 and 300 K were measured at DESY (Germany) [7, 25] and those at 400, 500, and 600 K were measured at SLRI (Thailand) [26].

T [K]	$\sigma^{(1)}$ [Å]		σ^2 [Å^2]		$\sigma^{(3)}$ [Å^3]		$\sigma^{(4)}$ ($\times 10^{-4}$) [Å^4]	
	present	expt.	present	expt.	present	expt.	present	expt.
77	0.0053	0.0053	0.0041	0.0041	0.0001	0.0001	0.0180	0.0180
300	0.0139	0.0141	0.0109	0.0109	0.0003	0.0003	0.1458	0.1460
400	0.0184	0.0190	0.0143	0.0149	0.0005	0.0006	0.3142	0.3144
500	0.0230	0.0236	0.0177	0.0185	0.0008	0.0009	0.5867	0.5869
600	0.0275	0.0284	0.0215	0.0223	0.0011	0.0012	0.9835	0.9837

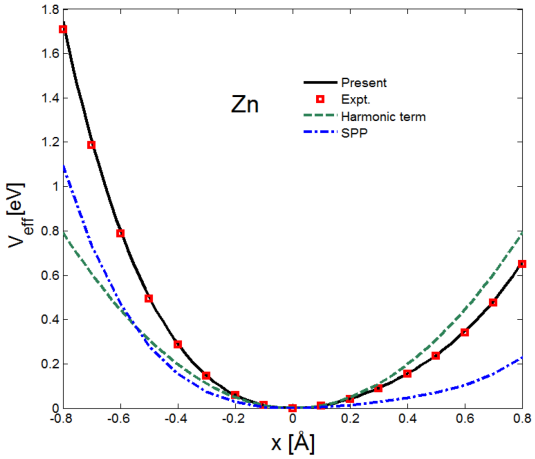

Fig. 1. Anharmonic many-body effect effective potential $V_{\rm eff}(x)$ of Zn calculated using the present theory (SCACEM) compared to its harmonic term, to the experimental values (expt.) [25], and to SPP.

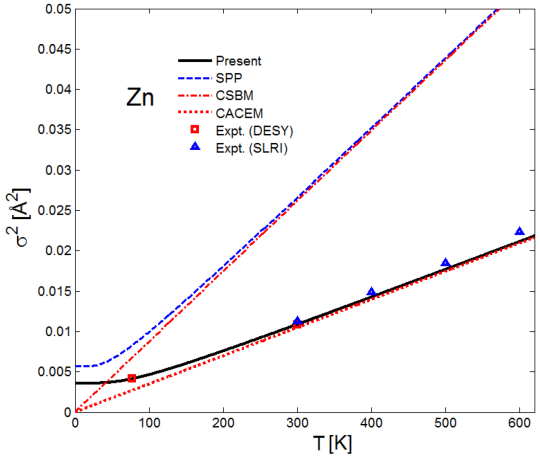

Fig. 2. Temperature-dependent second cumulant $\sigma^2(T)$ of Zn calculated using the present theory (SCACEM) compared to those calculated using SPP, CSBM [3], CACEM, and to the experimental values (expt.) measured at DESY [7, 25] and at SLRI [26].

Table II illustrates a good agreement of the values of four first cumulants $\sigma^{(1)}$ [Å], σ^2 [Å^2], $\sigma^{(3)}$ [Å^3], $\sigma^{(4)}$ [Å^4] of Zn calculated using the present theory (SCACEM) with their experimental values (expt.) at 77, 300, 400, 500, 600 K. The experimental values at 77 and 300 K were measured at DESY (Germany) [7, 25], and those at 400, 500, and 600 K were measured at SLRI (Thailand) [26]. The values of the cumulants measured at SLRI at 300 K are equal to those measured at DESY at the same temperature.

Figure 2 shows good agreement of temperature-dependent second cumulant $\sigma^2(T)$ or MSRD of Zn calculated using the present theory (SCACEM) with the experimental values (expt.) measured at HASYLAB (DESY, Germany) [7, 25] and at SLRI (Thailand) [26], as well as its significant difference from those calculated with CSBM [3] and with the present theory using SPP.

Based on the advantage of the created method presenting all considered quantities in terms of second cumulant and $\sigma^2(T)$ computed by the present SCACEM (Fig. 2), the temperature-dependent first $\sigma^{(1)}(T)$, third $\sigma^{(3)}(T)$, and fourth $\sigma^{(4)}(T)$ cumulants have been obtained and are presented in Figs. 3, 4, and 5, respectively. They have been found to be in good agreement with the experimental values (expt.) measured at DESY [7, 25] and at SLRI [26], as well as significantly different from those calculated with CSBM [3] and the present theory using SPP.

Moreover, the first cumulant $\sigma^{(1)}$(T) describes the net thermal expansion or lattice disorder of a considered crystal so that it can also be used for obtaining temperature dependence of the atomic near-neighbor distance based on the expression $R(T) = R(0) + \sigma^{(1)}(T)$ [9] providing the same good agreement with experiments as for $\sigma^{(1)}(T)$.

The significant discrepancies of the second, first, third, and fourth cumulants of Zn calculated by CSBM [3] and by the present CACEM using the SPP parameters presented in Figs. 2–5, respectively, from the experimental values can be attributed to neglecting the many-body effects in SPP. Actually, the local force constant $k_{SP} = 15.8247$ N/m (Table I) calculated using SPP is

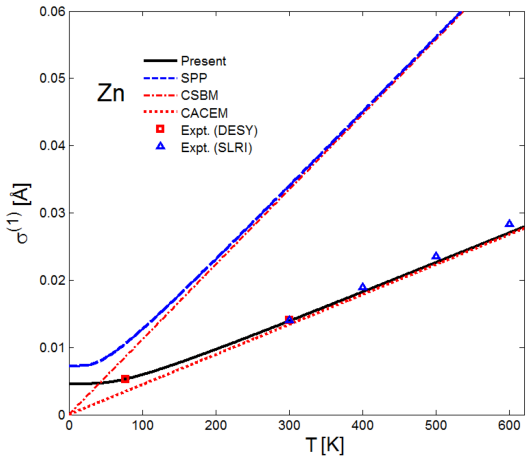

Fig. 3. Temperature-dependent first cumulant $\sigma^{(1)}(T)$ of Zn calculated using the present theory (SCACEM) compared to those calculated using SPP, CSBM [3], CACEM, and to the experimental values (expt.) measured at DESY [7, 25] and at SLRI [26].

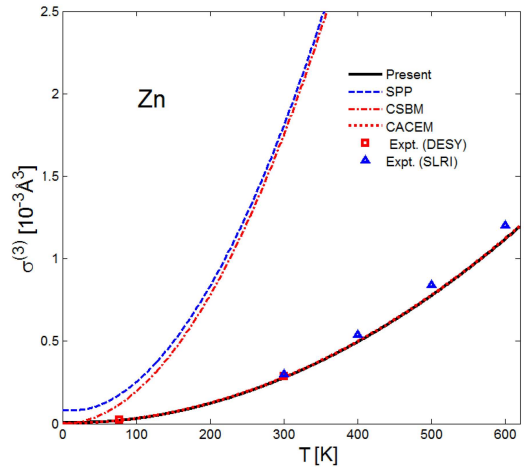

Fig. 4. Temperature-dependent third cumulant $\sigma^{(3)}(T)$ of Zn calculated using the present theory (SCACEM) compared to those calculated using SPP, CSBM [3], CACEM, as well as to the experimental values (expt.) measured at DESY [7, 25] and at SLRI [26].

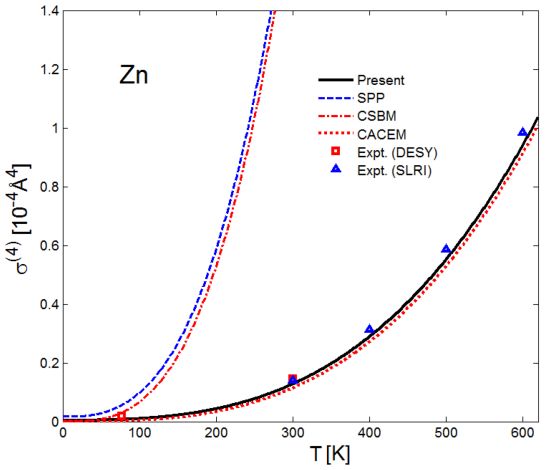

Fig. 5. Temperature-dependent fourth cumulant $\sigma^{(4)}(T)$ of Zn calculated using the present theory (SCACEM) compared to those calculated using SPP, CSBM [3], CACEM, and to the experimental values (expt.) measured at DESY [7, 25] and at SLRI [26].

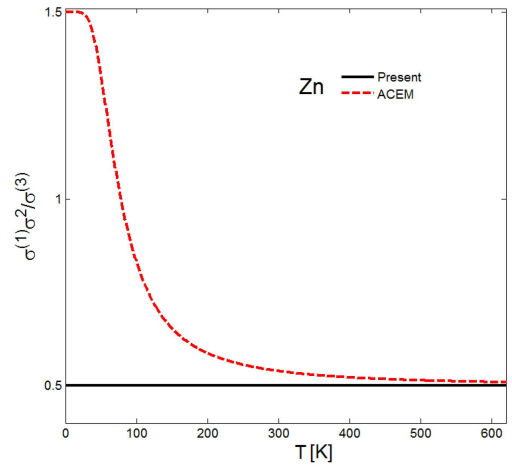

Fig. 6. Comparison of temperature-dependent cumulant relation $\sigma^{(1)}\sigma^2/\sigma^{(3)}$ of Zn calculated using the present theory (SCACEM) with the one calculated using the quantum ACEM [25].

significantly smaller than the one needed to approximate the observed phonon spectra. This indicates the limitations of the SPP model and the possible importance of the next-neighbor interactions describing the many-body effect included in the present theory (SCACEM) for hcp crystals. This SCACEM provides the larger value $k_{\text{eff}} = 39.5616$ N/m (Table I), leading to a good agreement of the EXAFS results of Zn calculated using the present theory (SCACEM) with the experimental values illustrated in the above figures.

The cumulants of Zn calculated using the present CACEM presented in the above figures provide, due to including the many-body effects, a good agreement with the experimental values but only at high temperatures and not at low temperatures because of the absence of zero-point vibration. Unfortunately, since the zero-point energy contributions of the third and fourth cumulants are negligibly small, this limitation has no important influence on these cumulants.

The cumulant relation $\sigma^{(1)}\sigma^2/\sigma^{(3)}$ is often considered in EXAFS cumulant studies, for example, in [3, 11, 15, 25, 26]. Figure 6 illustrates a comparison of temperature-dependent $\sigma^{(1)}\sigma^2/\sigma^{(3)}$ of Zn calculated using the present theory (SCACEM) with the one calculated by the quantum ACEM [25]. It is interesting that this obtained SCACEM cumulant relation is equal to the classical value of 1/2 at all

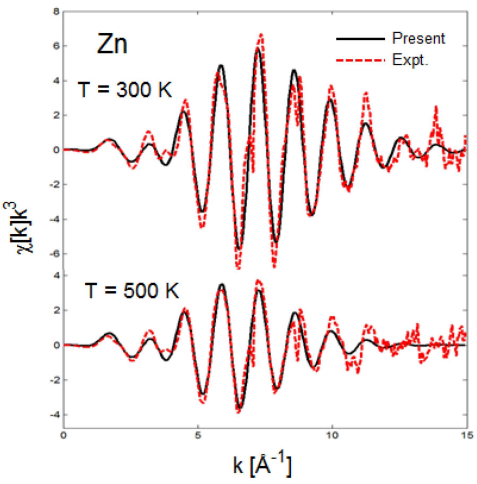

Fig. 7. Comparison of EXAFS spectra of Zn at 300 and 500 K calculated using the present theory (SCACEM) with the experimental values (expt.) [26].

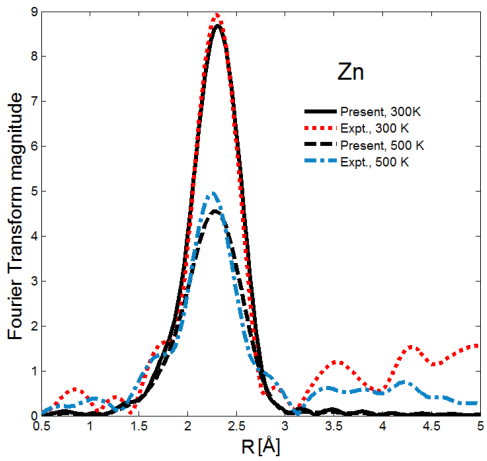

Fig. 8. Comparison of the Fourier transform magnitudes of EXAFS spectra at 300 K and 500 K calculated using the present theory (SCACEM) presented in Fig. 7 with the experimental values (expt.) [26].

temperatures for any classical model like the well-known CSBM [3], expressing a classical effect, while the first, second, and third cumulants (Figs. 3, 2, 4) contained in this relation include the zero-point energy contributions, i.e., a quantum effect. Therefore, this result confirms the special character of SCACEM that it includes both classical and quantum effects.

In EXAFS theory, EXAFS spectra and their Fourier transform magnitudes provide the structural determination [1], so the above cumulants or high-order expanded DWFs obtained using the present SCACEM are applied to studying the anharmonic EXAFS data of Zn. The calculations of these EXAFS spectra are carried out based on the FEFF code [27] with the modifications using (15), including the anharmonic contributions to the EXAFS amplitude given by (16) and its phase given by (17). Figure 7 illustrates the good agreement of EXAFS spectra of Zn at 300 K and 500 K calculated using the present theory (SCACEM) with their experimental values [26]. These obtained spectra have been Fourier-transformed also by this modified FEFF code. Their magnitudes are presented in Fig. 8 and for the first shell are found to be in good agreement with the experimental values (expt.) [26]. The above good results apparently demonstrate the important contributions of SCACEM to the accurate structural determination of hcp crystals. Note that, being different from the harmonic model, the EXAFS spectra and their Fourier transform magnitudes of Zn obtained by the present SCACEM are damped and shifted when the temperature changes from 300 to 500 K due to the anharmonic effects given by the obtained cumulants.

5. Conclusions

In this work, SCACEM of hcp crystals has been derived by combining the classical and quantum theories for the calculation and analysis of the high-order expanded DWFs, anharmonic EXAFS spectra and their Fourier transform magnitudes, which include not only the dominant anharmonicity at high temperatures, the advantage of classical theory, but also the zero-point energy contributions at low temperatures, the advantage of quantum theory.

The present SCACEM has successfully simplified the problem of the many-body system in EXAFS theory into one of the linear anharmonic oscillator models by taking the many-body effect into account in a simple manner based on the contributions of the first shell near neighbors of absorber and backscatter atoms where the Morse potential is used for describing the single-pair atomic interactions.

The advantageous development of this SCACEM has been the creation of a method giving the best way for providing all considered quantities, correcting the absence of zero-point vibration of the classical theory of EXAFS, and combining it with the quantum one based on only the second cumulant or MSRD. This also illustrates the close relation of the thermodynamic properties and anharmonic effects of hcp crystals with their atomic displacements, as well as leads to the significant reduction and simplification of the numerical calculations of the considered quantities.

The significant discrepancies between the considered EXAFS quantities of Zn calculated with CSBM and with the present theory using the SPPs from the experimental values indicate the limitations of the SPP model and the importance of including the many-body effect in the present theory (SCACEM) providing good agreement of the calculated results with their experimental values.

The equality of the SCACEM cumulant relation $\sigma^{(1)}\sigma^2/\sigma^{(3)}$ to the classical value of 1/2 at all temperatures, while the cumulants included in this relation contain zero-point energy contributions, demonstrates the advantage of SCACEM of including both classical and quantum effects. This explains the reason for calling the derived model SCACEM opening up new possibilities in EXAFS theory for studying the thermodynamic properties and anharmonic effects, as well as for improving the accurate structural determination of the considered crystals at any temperature.

The present derived SCACEM avoids the intensive FLD calculations usually required by a task of a many-body system yet provides good agreement of the numerical results for all considered quantities of Zn in hcp phase with the experimental values. This illustrates the simplicity, advantages, efficiencies, and reliability of the present SCACEM in researching the high-order expanded DWFs, EXAFS spectra and their Fourier transform magnitudes of the considered hcp crystals, as well as those of the other structures based on calculating their anharmonic effective potential parameters.

Acknowledgments

The authors thank J.J. Rehr and P. Fornasini for their useful comments and suggestions.

References

[1] E.D. Crozier, J.J. Rehr, R. Ingalls, in: *X-ray Absorption: Principles, Applications, Techniques of EXAFS, SEXAFS and XANES*, Wiley, New York 1988, Ch. 9, p. 373.

[2] J.M. Tranquada, R. Ingalls, *Phys. Rev. B* **28**, 3520 (1983).

[3] E.A. Stern, P. Livins, Zhe Zhang, *Phys. Rev. B* **43**, 8850 (1991).

[4] N.V. Hung, R. Frahm, *Physica B* **208** & **209** 91, (1995).

[5] N.V. Hung, R. Frahm, H. Kamitsubo, *J. Phys. Soc. Jpn.* **65**, 3571 (1996).

[6] N.V. Hung, *J. de Physique* **IV**, C2-279 (1997).

[7] N.V. Hung, T.S. Tien, N.B. Duc, D.Q. Vuong, *Mod. Phys. Lett. B* **28**, 1450174 (2014).

[8] A.I. Frenkel and J.J. Rehr, *Phys. Rev. B* **48**, 585 (1993).

[9] T. Yokoyama, K. Kobayashi, T. Ohta, A. Ugawa, *Phys. Rev. B* **53**, 6111 (1996).

[10] T. Miyanaga, T. Fujikawa, *J. Phys. Soc. Jpn.* **63**, 1036 and 3683 (1994).

[11] N.V. Hung, J.J. Rehr, *Phys. Rev. B* **56**, 43 (1997).

[12] N.V. Hung, *J. Phys. Soc. Jpn.* **83**, 024802 (2014).

[13] M. Daniel, D.M. Pease, N.V. Hung, J.I. Budnick, *Phys. Rev. B* **69**, 134414 (2004).

[14] N.V. Hung, N.B. Duc, D.Q. Vuong, T.S. Tien, N.C. Toan, *Rad. Phys. Chem.* **80**, 109263 (2021).

[15] N.V. Hung, C.S. Thang, N.C. Toan, H.K. Hieu, *VAC* **101**, 63 (2014).

[16] N.V. Hung, N.B. Duc, D.Q. Vuong, N.C. Toan, T.S. Tien, *VAC* **169**, 108872 (2019).

[17] T. Yokoyama, *Phys. Rev. B* **57**, 3423 (1998).

[18] A.V. Poiarkova, J.J. Rehr, *Phys. Rev. B* **59**, 948 (1999).

[19] R.M. Niclow, G. Gilat, H.G. Smith, L.J. Raubenheimer, M.K. Wilkinson, *Phys. Rev.* **164**, 922 (1967).

[20] S. a Beccara, G. Dalba, P. Fornasini, R. Grisenti, F. Pederiva, A. Samson, *Phys. Rev. B* **68**, 140301(R) (2003).

[21] F.D. Vila, J.J. Rehr, H.H. Rossner, H.J. Krappe, *Phys. Rev. B* **76**, 014301 (2007).

[22] C. Malica, A. Dal Corso, *Acta Cryst. A* **75**, 624 (2019).

[23] P. Wu, K. Xia, K. Peng et al., *Phys. Rev. B* **103**, 195204 (2021).

[24] N.C. Toan, D.Q. Vuong, N.V. Hung, *Acta Phys. Pol. A* **140**, 27 (2021).

[25] N.V. Hung, T.S. Tien, L.H. Hung, R.R. Frahm, *Int. J. Mod. Phys. B* **22**, 5155 (2008).

[26] N.V. Hung, C.S. Thang, N.B. Duc, D.Q. Vuong, T.S. Tien, *Phys. B* **521**, 198 (2017).

[27] J.J. Rehr, J. Mustre de Leon, S.I. Zabinsky, R.C. Albers, *J. Am. Chem. Soc.* **113**, 5135 (1991).

[28] N.V. Hung, *Commun. Phys. (CIP)* **14**, 7 (2004).